Physics Letters B 738 (2014) 223–227

Contents lists available at ScienceDirect

Physics Letters B

www.elsevier.com/locate/physletb

Identification of a millisecond isomeric state in $^{129}Cd_{81}$ via the detection of internal conversion and Compton electrons

J. Taprogge[a,b,c], A. Jungclaus[a,*], H. Grawe[d], S. Nishimura[c], Z.Y. Xu[c], P. Doornenbal[c], G. Lorusso[c], E. Nácher[a], G.S. Simpson[e], P.-A. Söderström[c], T. Sumikama[f], H. Baba[c], F. Browne[h,c], N. Fukuda[c], R. Gernhäuser[i], G. Gey[e,j,c], N. Inabe[c], T. Isobe[c], H.S. Jung[k,1], D. Kameda[c], G.D. Kim[l], Y.-K. Kim[l,m], I. Kojouharov[d], T. Kubo[c], N. Kurz[d], Y.K. Kwon[l], Z. Li[n], H. Sakurai[c,g], H. Schaffner[d], K. Steiger[i], H. Suzuki[c], H. Takeda[c], Zs. Vajta[o,c], H. Watanabe[c], J. Wu[n,c], A. Yagi[p], K. Yoshinaga[q], G. Benzoni[r], S. Bönig[s], K.Y. Chae[t], L. Coraggio[u], A. Covello[v], J.-M. Daugas[w], F. Drouet[e], A. Gadea[x], A. Gargano[u], S. Ilieva[s], F.G. Kondev[y], T. Kröll[s], G.J. Lane[z], A. Montaner-Pizá[x], K. Moschner[aa], D. Mücher[s], F. Naqvi[ab], M. Niikura[g], H. Nishibata[p], A. Odahara[p], R. Orlandi[ac,ad], Z. Patel[ae], Zs. Podolyák[ae], A. Wendt[aa]

[a] Instituto de Estructura de la Materia, CSIC, E-28006 Madrid, Spain
[b] Departamento de Física Teórica, Universidad Autónoma de Madrid, E-28049 Madrid, Spain
[c] RIKEN Nishina Center, RIKEN, 2-1 Hirosawa, Wako-shi, Saitama 351-0198, Japan
[d] GSI Helmholtzzentrum für Schwerionenforschung GmbH, 64291 Darmstadt, Germany
[e] LPSC, Université Joseph Fourier Grenoble 1, CNRS/IN2P3, Institut National Polytechnique de Grenoble, F-38026 Grenoble cedex, France
[f] Department of Physics, Tohoku University, Aoba, Sendai, Miyagi 980-8578, Japan
[g] Department of Physics, University of Tokyo, Hongo 7-3-1, Bunkyo-ku, 113-0033 Tokyo, Japan
[h] School of Computing, Engineering and Mathematics, University of Brighton, Brighton BN2 4JG, United Kingdom
[i] Physik Department E12, Technische Universität München, D-85748 Garching, Germany
[j] Institut Laue-Langevin, B.P. 156, F-38042 Grenoble cedex 9, France
[k] Department of Physics, Chung-Ang University, Seoul 156-756, Republic of Korea
[l] Rare Isotope Science Project, Institute for Basic Science, Daejeon 305-811, Republic of Korea
[m] Department of Nuclear Engineering, Hanyang University, Seoul 133-791, Republic of Korea
[n] School of Physics and State Key Laboratory of Nuclear Physics and Technology, Peking University, Beijing 100871, China
[o] MTA Atomki, P.O. Box 51, Debrecen H-4001, Hungary
[p] Department of Physics, Osaka University, Machikaneyama-machi 1-1, Osaka 560-0043, Toyonaka, Japan
[q] Department of Physics, Faculty of Science and Technology, Tokyo University of Science, 2641 Yamazaki, Noda, Chiba, Japan
[r] INFN, Sezione di Milano, via Celoria 16, I-20133 Milano, Italy
[s] Institut für Kernphysik, Technische Universität Darmstadt, D-64289 Darmstadt, Germany
[t] Department of Physics, Sungkyunkwan University, Suwon 440-746, Republic of Korea
[u] Istituto Nazionale di Fisica Nucleare, Complesso Universitario di Monte S. Angelo, I-80126 Napoli, Italy
[v] Dipartimento di Fisica, Università di Napoli Federico II, Complesso Universitario di Monte S. Angelo, I-80126 Napoli, Italy
[w] CEA, DAM, DIF, 91297 Arpajon cedex, France
[x] Instituto de Física Corpuscular, CSIC-Univ. of Valencia, E-46980 Paterna, Spain
[y] Nuclear Engineering Division, Argonne National Laboratory, Argonne, IL 60439, USA
[z] Department of Nuclear Physics, Research School of Physical Sciences and Engineering, Australian National University, Canberra, ACT 0200, Australia
[aa] IKP, University of Cologne, D-50937 Cologne, Germany
[ab] Wright Nuclear Structure Laboratory, Yale University, New Haven, CT 06520-8120, USA
[ac] Instituut voor Kern- en Stralingsfysica, K.U. Leuven, B-3001 Heverlee, Belgium
[ad] Advanced Science Research Center, Japan Atomic Energy Agency, Tokai, Ibaraki 319-1195, Japan
[ae] Department of Physics, University of Surrey, Guildford GU2 7XH, United Kingdom

* Corresponding author.
E-mail address: andrea.jungclaus@csic.es (A. Jungclaus).
[1] Present address: Department of Physics, University of Notre Dame, Notre Dame, IN 46556, USA.

http://dx.doi.org/10.1016/j.physletb.2014.09.047

A R T I C L E I N F O

Article history:
Received 23 June 2014
Received in revised form 8 September 2014
Accepted 20 September 2014
Available online 26 September 2014
Editor: V. Metag

Keywords:
Isomeric decays
Transition strengths
Shell model calculations

A B S T R A C T

The decay of an isomeric state in the neutron-rich nucleus ^{129}Cd has been observed via the detection of internal conversion and Compton electrons providing first experimental information on excited states in this nucleus. The isomer was populated in the projectile fission of a ^{238}U beam at the Radioactive Isotope Beam Factory at RIKEN. From the measured yields of γ-rays and internal conversion electrons, a multipolarity of $E3$ was tentatively assigned to the isomeric transition. A half-life of $T_{1/2} = 3.6(2)$ ms was determined for the new state which was assigned a spin of $(21/2^+)$, based on a comparison to shell model calculations performed using state-of-the-art realistic effective interactions.

The spectroscopy of isomeric states near nuclear shell closures provides a very sensitive tool to study the evolution of single-particle levels. In the region around double-magic ^{132}Sn one of the most important topics is the evolution of the $N = 82$ shell gap below ^{132}Sn towards ^{122}Zr, which is crucial also for nuclear astrophysics and in particular the description of the rapid-neutron capture process. This evolution depends in part on the behavior of the neutron $0h_{11/2}$ orbital which for $Z < 50$ is located directly below the $N = 82$ gap. The question is how the energy of this orbital varies when protons are successively removed from the $0g_{9/2}$, $1p_{1/2}$, $1p_{3/2}$, and $0f_{5/2}$ orbitals along $N = 82$ towards the neutron drip line.

The alignment of two $0g_{9/2}$ protons or two $0h_{11/2}$ neutrons gives rise to the formation of isomeric states, the so-called seniority isomers, which are observed as 8^+ states in the $N = 82$ isotones ^{130}Cd and ^{128}Pd [1,2] and 10^+ states in several Sn isotopes [3]. Relatively pure three-quasiparticle states containing both $0g_{9/2}$ protons and $0h_{11/2}$ neutrons are expected in the odd-proton nucleus ^{129}In and the odd-neutron analog ^{129}Cd. In ^{129}In, a candidate for the $29/2^+$ state with fully aligned $\pi(g_{9/2}^{-1})\nu(h_{11/2}^{-2})$ configuration was identified, decaying via an $E3$ transition of 281 keV with a half-life of 110(15) ms [4]. In addition, the decay of a $17/2^-$ isomer with $T_{1/2} = 8.5(5)$ μs was reported in Ref. [5]. In ^{129}Cd, on the other hand, no isomeric state has been identified so far, actually no excited state at all is experimentally known. Microsecond isomers in this nucleus have been searched for in an experiment performed some years ago at GSI (Darmstadt) during the RISING campaign. In that experiment a large number of isomers were identified in neutron-rich Ag, Cd, In and Sn isotopes [1,6–10], among them in $^{125-128}$Cd and ^{130}Cd. However, although about 5×10^4 ^{129}Cd ions were identified, no delayed γ-rays were observed at that time [11]. It was the aim of the present work to identify for the first time excited states in the nucleus ^{129}Cd decaying either via the emission of γ-rays or via β-decay. As a tool for this purpose decay spectroscopy was performed using a Si array as active stopper and a highly-efficient γ-ray spectrometer.

The experiment was performed at the Radioactive Isotope Beam Factory (RIBF) of the RIKEN Nishina Center. The neutron-rich ^{129}Cd nuclei were produced following the projectile fission of a 345 MeV/u ^{238}U beam with an average intensity of about 8 pnA, impinging on a 3-mm thick Be target. The ions of interest were separated from other reaction products and identified on an ion-by-ion basis by the BigRIPS in-flight separator [12]. The particle identification was performed using the ΔE-TOF-$B\rho$ method in which the energy loss (ΔE), time of flight (TOF) and magnetic rigidity ($B\rho$) are measured and used to determine the atomic number, Z, and the mass-to-charge ratio, A/q, of the fragments. Details about the identification procedure can be found in Ref. [13]. Two different settings of BigRIPS were used, one optimized for the maximum transmission of ^{136}Sn and the other one tuned to predominantly transmit ^{128}Pd. In total about 3.2×10^6 ^{129}Cd ions were identified, transported through the ZeroDegree spectrometer (ZDS) and finally implanted into the WAS3ABi (Wide-range Active Silicon Strip Stopper Array for β and ion detection) Si array positioned at the F11 focal plane of the ZDS. The WAS3ABi detector [14–17] consists of eight closely packed DSSSD (double-sided silicon strip detectors) with an area of 60×40 mm^2, a thickness of 1 mm and a segmentation of 40 horizontal and 60 vertical strips each. All decay events detected in WAS3ABi were stored and correlated off-line in space and time with the implanted ions. To detect γ radiation emitted following the decay of the implanted radioactive nuclei 12 large-volume Ge Cluster detectors [18] from the former EUROBALL spectrometer [19] were arranged in a close geometry around the WAS3ABi detector.

In a first step of the analysis the spectrum of the time difference between the implantation of a ^{129}Cd ion and a successive decay signal detected at the same position in the Si detectors was inspected. Clearly a component with a very short decay time in the range of a few milliseconds was observed which cannot be assigned to the two known β-decaying states with half-lives of 104(6) and 242(8) ms, respectively, reported by Arndt et al. [20]. To uncover the origin of this new decay component we explored the Si energy spectra shown in Fig. 1(a) created for the first 10 ms and the time range 30–40 ms after an ion implantation. While the spectrum for the later time interval shows the smooth energy distribution expected for β-decay events, the spectrum for the decays occurring during the first few ms after implantation clearly exhibits peak-like structures at energies of about 340 and 390 keV. In addition a closer inspection also reveals an excess of intensity in the region below 250 keV in this spectrum. Requiring that energy was deposited exclusively in the Si detector in which the ion was implanted, see Fig. 1(b), the continuous contribution to the energy distribution is strongly reduced and it becomes evident that predominantly particles with energies below 430 keV are emitted in the fast decay component. Another important observation from Fig. 1 is that the strong peak at around 340 keV seems to have a doublet structure.

The spectra of γ-rays emitted in prompt coincidence with particles with energies in the two ranges 295–430 keV respectively < 250 keV are shown in Fig. 2(a) and (b). Only those decay events, in which energy was deposited exclusively in the same Si detector as that in which the ion was implanted (same condition as in Fig. 1(b)), were considered. To remove the contributions from β-decay events, the γ-ray spectra obtained in the time interval 30–40 ms after the implantation were subtracted from the ones created for the first 10 ms. Four lines at energies of 353, 406, 1181, and 1587 keV are visible in both spectra. However, the intensity ratio between the 353 and 406 keV lines is clearly different. While they are observed with similar intensity in coincidence with particles in the energy range below 250 keV, compare Fig. 1(b), the

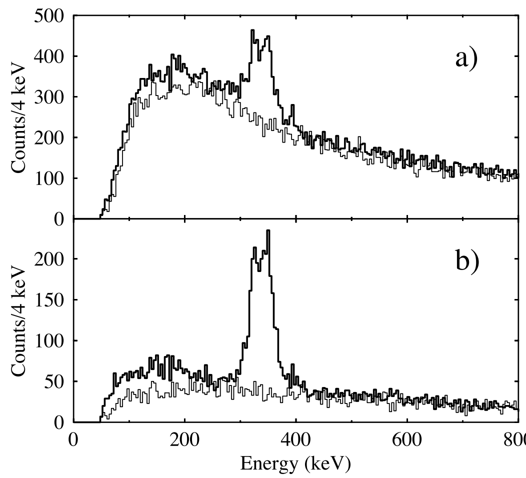

Fig. 1. Energy spectra of decay events registered in the Si detectors in the first 10 ms after the implantation of a ^{129}Cd ion (thick lines) and in the range 30–40 ms after implantation (thin lines): a) without additional condition and b) considering only those decay events in which energy was deposited exclusively in the Si detector in which the ion was implanted.

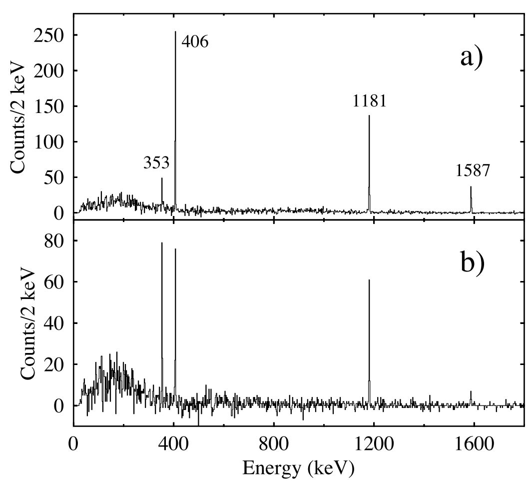

Fig. 2. Two γ-ray spectra in prompt coincidence with a decay event registered in the first 10 ms after an implantation for a) the particle energy range 295–430 keV corresponding to internal conversion electrons and b) the particle energy range < 250 keV corresponding to Compton electrons.

353 keV line is strongly suppressed in comparison to the 406 keV line when gating on the two peaks at around 340 and 390 keV, compare Fig. 1(a). This observation suggests that the energy region below 250 keV corresponds to Compton electrons while the broad peaks at higher energies are produced by internal conversion electrons emitted in the 353 keV and, to a lesser extent, 406 keV transitions. The half-life of the short-lived decay component was obtained from the summed time difference distribution ($t_{decay} - t_{ion}$) of the 406 and 1181 keV γ-rays, resulting in a value of $T_{1/2} = 3.6(2)$ ms.

To summarize, the experimental observations indicate the existence of a new isomeric state in ^{129}Cd with a half-life in the millisecond range which decays via the emission of the four γ rays listed above, the first two of them being partially converted. It is then either these internal conversion electrons which deposit energy in the Si detectors and thus lead to the registration of a decay event or electrons originating from the Compton scattering of these γ rays in the Si detector. From the intensities of the 353 and 406 keV lines in the spectrum shown in Fig. 2(a) it can be deduced that the internal conversion coefficient of the 353 keV

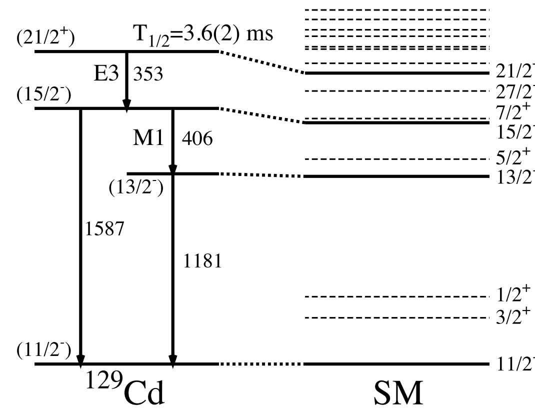

Fig. 3. Proposed decay scheme of the new isomeric state in ^{129}Cd in comparison to shell model calculations (see text for details).

transition is larger by a factor of about six as compared to that of the 406 keV transition. The coincidence relations between the four observed γ-rays suggest a decay scheme as shown in Fig. 3 with the 406–1181 keV cascade in parallel to the 1587 keV transition. Note that the order within the cascade cannot be fixed solely on the basis of the available experimental information. Considering the factor six difference in internal conversion coefficients between the 353 and 406 keV transitions the most probable multipolarity assignments are $M2$ ($\alpha = 0.0626$) or $E3$ ($\alpha = 0.0665$) for the 353 keV and $M1$ ($\alpha = 0.0111$) or $E2$ ($\alpha = 0.0124$) for the 406 keV transition (all internal conversion coefficients were calculated with the aid of Ref. [21]). A higher multipolarity of the 353 keV transition would imply an unreasonably high multipolarity of the 406 keV transition considering the existence of the parallel decay branch.

To prove this scenario Monte Carlo simulations were performed using the Geant4 package [22]. The stack of Si detectors as well as the Ge array have been included in the geometry and events were generated according to the decay scheme shown in Fig. 3. Fig. 4 shows a comparison between the simulated and experimental spectra corresponding to the energy deposited in the Si detector in coincidence with the 406, 1181, and 353 keV γ-rays detected in the Ge array. In the simulations an energy resolution of 20–25 keV was assumed for the Si detectors in the relevant energy range. Although the statistics are limited an overall good agreement is found over the full energy range including the Compton part. Furthermore the simulations allow us to disclose the origin of the double-peak structure already observed in the Si energy projections shown in Fig. 1. In Fig. 4(a) simulated energy distributions without smearing are included considering either only the internal conversion electrons or including in addition also the subsequently emitted X-rays. In the first case the K and L (and higher) internal conversion electrons are visible with an intensity ratio of roughly 4:1 as expected. In the second the partial summing of electron and X-ray energies gives rise to a shift of the peaks and also to a redistribution of the intensity which finally leads to the observed double-peak structure. Note that the K_α X-ray has an energy of about 23 keV and therefore a considerable probability to escape the Si layer.

We would like to point out that to our knowledge this is the first unambiguous case of the establishment of an isomeric decay in the millisecond range on the basis of the detection of internal conversion and Compton electrons in an active stopper.

The observed decay sequence is compared to shell model calculations (SM) in Fig. 3. These calculations employ a two-body effective interaction derived from the CD-Bonn nucleon–nucleon potential renormalized by way of the $V_{low\text{-}k}$ approach [23]. Specifically,

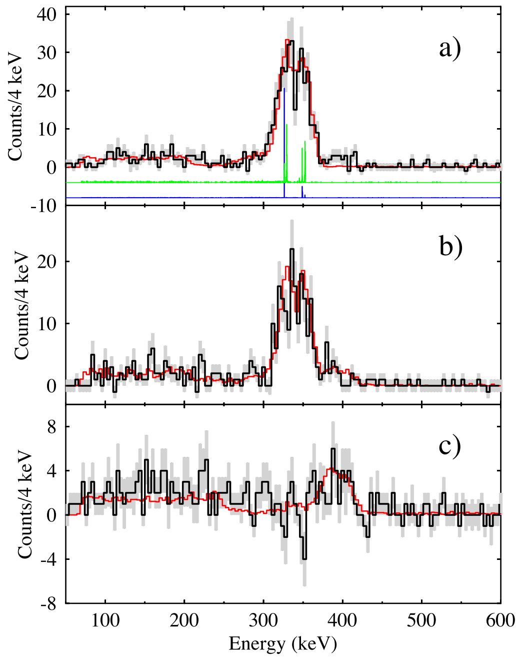

Fig. 4. (Color online.) Energy spectra of decay events registered in the Si detectors in the first 10 ms after an implantation in coincidence with a) the 406 keV, b) the 1181 keV and c) the 353 keV γ-ray detected in the EURICA array. The experimental spectra are shown as black lines (with the uncertainty given as grey areas) while the results of Monte Carlo simulations are shown as red lines (see text for details). In part (a) the simulated spectra are shown before folding in the detector response considering only internal conversion electrons (blue line) or in addition also successive X-ray cascades (green line). The latter two spectra are shown with an offset to provide a better legibility of the figure.

the interaction is constructed by assuming ^{132}Sn as closed core and considering the full $N = 50$–82 major shell for neutrons (i.e. the $0g_{7/2}$, $1d_{5/2}$, $1d_{3/2}$, $2s_{1/2}$ and $0h_{11/2}$ orbitals) and the $Z = 28$–50 shell for protons (i.e. the $0f_{5/2}$, $1p_{3/2}$, $1p_{1/2}$ and $0g_{9/2}$ orbits). The neutron single-particle energies were taken from Ref. [24], while for the protons energies of 0.365 ($1p_{1/2}$) and 1.353 MeV ($1p_{3/2}$) relative to the $0g_{9/2}$ orbital as reported from very recent mass measurements and decay spectroscopy, respectively, were employed [25,26]. For the experimentally still unknown energy of the $0f_{5/2}$ proton orbital a value of 2.6 MeV relative to $0g_{9/2}$ was adopted to be consistent with the shell model calculations presented in Ref. [26] in which further details on the interaction are given. Besides a reduction of the $\pi\pi$ pairing to 88% the modifications comprised an increase of the $\nu\nu$ and $\pi\nu$ multipoles by factors of 1.6 and 1.5 in the dominant configurations $\nu h^2_{11/2}$ and $\nu h_{11/2}\pi g_{9/2}$. As the largest multipole part is quadrupole this increases $L = 2$ collectivity. The modified interaction yields a good description of the $^{125-130}$Sn isotopes as compiled in Ref. [27] and recent experimental data in ^{127,128,130}Cd [8,7,1] and ^{126,128}Pd [2]. Effective charges $e_\pi = 1.5e$, $e_\nu = 0.7e$ for $E2$ and $E3$ and effective spin g-factors $g_s = 0.7g_s^{free}$ for $M1$ transitions were used. Calculations were performed with the code OXBASH [28].

The shell model calculations predict the existence of two isomeric states in ^{129}Cd, a $27/2^-$ level at an excitation energy of 1695 keV and a $21/2^+$ state about 100 keV higher at 1806 keV. The first is an $E6$ spin trap corresponding to the fully aligned coupling between two $0g_{9/2}$ proton and one $0h_{11/2}$ neutron holes and is expected to undergo β-decay. The $21/2^+$ state, on the other hand, involves a proton hole in a negative parity orbital and is predicted to decay via an $E3$ transition to the $15/2^-$ level. Also indicated in Fig. 3 is the position of low-spin positive-parity states which correspond to neutron single-hole states as well as a number of closely lying levels above the $21/2^+$ state with spins in the range 17/2–23/2 and both positive as well as negative parity. Note that none of these states is expected to be isomeric. Based on the comparison to the SM calculations shown in Fig. 3 we tentatively assign spin and parity of $(21/2^+)$ to the experimentally observed millisecond isomer. It decays via an $E3$ transition to the $(15/2^-)$ state and from there via two parallel branches down to the $(11/2^-)$ level which the SM calculation proposes to be the ground state, 287 keV below the beta-decaying $3/2^+$ state.

The electromagnetic transition strength of the $(21/2^+) \rightarrow (15/2^-)$ $E3$ transition depends sensitively on the position of the $1p_{3/2}$ proton orbital relative to that of the $1p_{1/2}$ state. In contrast the dependence on the exact $\pi 0f_{5/2}$ position is weak due to the small, since non-stretched, $f_{5/2} \rightarrow g_{9/2}$ reduced $E3$ matrix element. While the final state is built of the $\nu(h^{-1}_{11/2})\pi(g^{-2}_{9/2})$ configuration (corresponding to the coupling of the $h_{11/2}$ neutron hole to the $(2$–$8)^+$ states in ^{130}Cd), the positive parity of the initial state necessarily requires the involvement of a proton in one of the negative parity orbitals, namely $1p_{1/2}$, $1p_{3/2}$ or $0f_{5/2}$. Since the main partition of the wave function of the $(21/2^+)$ state, $\nu(h^{-1}_{11/2})\pi(g^{-1}_{9/2}p^{-1}_{1/2})$, cannot contribute to the $E3$ decay to the $\nu(h^{-1}_{11/2})\pi(g^{-2}_{9/2})$ state this transition only occurs due to the admixtures of the $\nu(h^{-1}_{11/2})\pi(g^{-1}_{9/2}p^{-1}_{3/2})$ and $\nu(h^{-1}_{11/2})\pi(g^{-1}_{9/2}f^{-1}_{5/2})$ configurations to the wave function. The amount of these admixtures, on the other hand, depends in part on the differences between the proton single-particle energies.

The experimentally determined half-life of the $(21/2^+)$ state, $T_{1/2} = 3.6(2)$ ms, implies a reduced transition strength of $B(E3) = 0.50(3)$ W.u. for the $E3$ transition to the $(15/2^-)$ level. This value can be compared to the one obtained from the shell-model calculation which however does not only depend on the wave functions of both the initial and final state but also on the effective charges assumed for this transition. Unfortunately the latter are poorly known since only a few $E3$ transitions are known in this region and furthermore most of them are very weak and therefore not well suited to constrain the effective charges. Assuming the values listed above the SM calculation results in a strength of $B(E3) = 0.48$ W.u., in perfect agreement with the experimental result. As mentioned above in the present work the new $1p_{3/2}$ energy established in recent experimental work [26] has been employed. To demonstrate the sensitivity of the $B(E3)$ strength to this value, we repeated the calculation adopting the single-particle energies suggested in Ref. [29]. In that work a significantly higher value of 1.65 MeV relative to the $0g_{9/2}$ orbit was proposed for the $1p_{3/2}$ orbit, while an energy of 2.75 MeV was listed for the $1f_{5/2}$ state. This implies a larger spin-orbit splitting of the $1p$ orbital of 1.28 MeV as compared to 0.99 MeV from Ref. [26] adopted in the present work. The use of these single-particle energies leads to a value of $B(E3) = 0.31$ W.u. for the $21/2^+ \rightarrow 15/2^-$ transition, in conflict with the experimental result.

While the dependence of the $E3$ strength on the single-particle energies is evident, the current ambiguity in the choice of the effective charges unfortunately prevents us from using this dependence to constrain the still unknown energy of the fourth proton state below ^{132}Sn, namely $1f_{5/2}$. Note, however, that once this energy will become available in the future, the strong $E3$ transition in ^{129}Cd will constitute a very sensitive case to fix the effective charges in this model space.

To further validate the SM calculations we consider for comparison the strongly hindered $19/2^+ \rightarrow 13/2^-$ $E3$ transition in ^{127}Cd whose transition probability, $B(E3) = 0.0340(18)$ W.u., was measured in Ref. [8]. The hindrance of this transition is reproduced in the present SM approach and its origin is traced back to the differing structure of the $19/2^+$ and $13/2^-$ vs. $21/2^+$ and $15/2^-$ wave

Table 1
Experimental and calculated (SM) $B(E3)$ values in W.u. for transitions in ^{127}Cd, ^{129}Cd, and ^{130}Cd which are driven by the $p_{3/2}^{-1} \to g_{9/2}^{-1}$ proton single-particle transition.

$I_1^\pi \to I_f^\pi$	^{127}Cd		^{129}Cd		^{130}Cd	
	exp.	SM	exp.	SM	$I_1^\pi \to I_f^\pi$	SM
$17/2^+ \to 11/2^-$	–	1.05	–	1.31	$3^- \to 0^+$	2.55
$19/2^+ \to 13/2^-$	0.034(2)[a]	0.0048	–	0.030	$4^- \to 2^+$	0.0013
$21/2^+ \to 15/2^-$	–	0.80	0.50(3)	0.47	$5^- \to 2^+$	0.27
$23/2^+ \to 17/2^-$	–	0.065	–	0.026	$6^- \to 4^+$	0.092

[a] From Ref. [8].

functions involved. Note that the strength of the corresponding, not yet observed, $19/2^+ \to 13/2^-$ transition in ^{129}Cd is calculated as $B(E3) = 0.030$ W.u., i.e. with comparable hindrance. The $21/2^+$ and $15/2^-$ states may be considered as stretched couplings between an $h_{11/2}$ neutron hole and the 5^- respectively 2^+ odd- and even-parity proton yrast states in ^{130}Cd. This enables a stretched $5^- \to 2^+$ $E3$ transition by virtue of a 4.5% $\pi g_{9/2}^{-1} p_{3/2}^{-1}$ partition in the $I^\pi = 5^-$ wave function. In contrast the $19/2^+$ and $13/2^-$ states are non-stretched couplings in the proton core states with additionally a dominating ^{130}Cd; 4^- configuration in the $19/2^+$ state. This $I^\pi = 4^-$ level, in contrast to the $I^\pi = 5^-$ state, carries less than 0.5% of the $\pi g_{9/2}^{-1} p_{3/2}^{-1}$ partition. This along with the non-stretched angular momentum recoupling accounts for the reduction of the $19/2^+ \to 13/2^-$ strength by more than one order of magnitude as compared to the $21/2^+ \to 15/2^-$ transition. This scenario is not reproduced with the original non-modified interaction, which yields $E3$ strengths of 0.32 W.u. and 0.84 W.u. for the $19/2^+ \to 13/2^-$ transition in ^{127}Cd and the $21/2^+ \to 15/2^-$ transition in ^{129}Cd, respectively. Thus the results of this discussion as summarized in Table 1 clearly corroborate the applied multipole modification of the $\pi\nu$ interaction. Note that the staggering of the stretched $E3$ strengths with spin corroborates the spin-parity assignment for the isomer. The contribution of the $\pi f_{5/2}^{-1} \to g_{9/2}^{-1}$ transition to the $E3$ is negligible as the corresponding non-stretched single-particle transition is reduced by an order of magnitude in comparison to the $\pi p_{3/2}^{-1} \to g_{9/2}^{-1}$ transition. The scenario basically persists if two more neutrons are removed in ^{127}Cd. Closing this discussion it is worth mentioning that the observed $M1/E2$ branching ratio for the decay of the $15/2^-$ state in ^{129}Cd, I(406 keV) : I(1587 keV) $\approx 3:1$, is well accounted for by the SM result of 2:1 with the present choice of interaction and effective operators as listed above.

To conclude we reported on the identification of an isomeric state with a half-life of $T_{1/2} = 3.6(2)$ ms in the nucleus ^{129}Cd, decaying via the emission of a γ-ray with multipolarity $E3$. We thus provided the first experimental information with respect to excited states in this nucleus. The decay was identified via the detection of internal conversion as well as Compton electrons in an active stopper. To our knowledge this is the first time that a γ-decaying millisecond isomer was established in this way. Based on the comparison to state-of-the-art shell model calculations we tentatively assigned spin/parity of $21/2^+$ to this state. The discussion of the systematic of $E3$ strengths with respect to the intrinsic structure of the wave functions clearly justifies the $\pi\nu$ multipole modification applied for level scheme energetics.

Acknowledgements

This experiment was performed at RI Beam Factory operated by RIKEN Nishina Center and CNS, University of Tokyo. We thank the staff of the accelerator complex for providing stable beams with high intensities to the experiment. We acknowledge the EUROBALL Owners Committee for the loan of germanium detectors and the PreSpec Collaboration for the readout electronics of the cluster detectors. This work was supported by the Spanish Ministerio de Ciencia e Innovación under contracts FPA2009-13377-C02 and FPA2011-29854-C04, the Generalitat Valenciana (Spain) under grant PROMETEO/2010/101, the Japanese government under contract KAKENHI (25247045), the National Research Foundation of Korea (NRF) grant funded by the Korea government (MEST) (No. NRF-2012R1A1A1041763), the Priority Centers Research Program in Korea (2009-0093817), OTKA contract number K-100835, the European Commission through the Marie Curie Actions call FP7-PEOPLE-2011-IEF under Contract No. 300096, the U.S. Department of Energy, Office of Nuclear Physics, under Contract No. DE-AC02-06CH11357, STFC (UK), and the German BMBF (Nos. 05P12RDCIA and 05P12RDNUP) and HIC for FAIR.

References

[1] A. Jungclaus, et al., Phys. Rev. Lett. 99 (2007) 132501.
[2] H. Watanabe, et al., Phys. Rev. Lett. 111 (2013) 152501.
[3] B. Fogelberg, K. Heyde, J. Sau, Nucl. Phys. A 352 (1981) 157.
[4] B. Fogelberg, et al., in: H. Faust, G. Fioni, S. Oberstedt, F.-J. Hambsch (Eds.), Nuclear Fission and Fission-Product Spectroscopy, in: AIP Conf. Proc., vol. 447, AIP, Woodbury, NY, 1998, p. 191.
[5] J. Genevey, et al., Phys. Rev. C 67 (2003) 054312.
[6] M. Górska, et al., Phys. Lett. B 672 (2009) 308.
[7] L. Cáceres, et al., Phys. Rev. C 79 (2009) 011301(R).
[8] F. Naqvi, et al., Phys. Rev. C 82 (2010) 034323.
[9] S. Pietri, et al., Phys. Rev. C 83 (2010) 044328.
[10] S. Lalkovski, et al., Phys. Rev. C 87 (2013) 034308.
[11] F. Naqvi, PhD thesis, Universität zu Köln, 2011.
[12] T. Kubo, Nucl. Instrum. Methods Phys. Res. B 204 (2003) 97.
[13] T. Ohnishi, et al., J. Phys. Soc. Jpn. 79 (2010) 073201.
[14] S. Nishimura, et al., Prog. Theor. Exp. Phys. 03C006 (2012).
[15] P.-A. Söderström, et al., Nucl. Instrum. Methods Phys. Res. B 317 (2013) 649.
[16] G. Lorusso, et al., AIP Conf. Proc. 1594 (2014) 370.
[17] J. Wu, et al., AIP Conf. Proc. 1594 (2014) 388.
[18] J. Eberth, et al., Nucl. Instrum. Methods Phys. Res. A 369 (1996) 135.
[19] J. Simpson, Z. Phys. A 358 (1997) 139.
[20] O. Arndt, et al., Acta Phys. Pol. B 40 (2009) 437.
[21] http://bricc.anu.edu.au/index.php.
[22] S. Agostinelli, et al., Nucl. Instrum. Methods Phys. Res. A 506 (2003) 250.
[23] L. Coraggio, et al., Prog. Part. Nucl. Phys. 62 (2009) 135.
[24] H. Grawe, K. Langanke, G. Martínez-Pinedo, Rep. Prog. Phys. 70 (2007) 1525.
[25] A. Kankainen, et al., Phys. Rev. C 87 (2013) 024307.
[26] J. Taprogge, et al., Phys. Rev. Lett. 112 (2014) 132501.
[27] http://www.nndc.bnl.gov/ensdf/.
[28] B.A. Brown, et al., OXBASH for windows, MSU-NSCL report 1289, 2004.
[29] M. Hannawald, et al., Phys. Rev. C 62 (2000) 054301.